

## Kinetic Study of Adsorption of Metal Ions (Iron and Manganese) in Groundwater Using Calcium Carbide Waste

Muhammad Arief Karim<sup>1\*</sup>, Subriyer Nasir<sup>2</sup>, Tri Wardani Widowati<sup>3</sup>, Udin Hasanudin<sup>4</sup>

<sup>1</sup> Department of Chemical Engineering, Faculty of Engineering, University of Muhammadiyah Palembang, Jalan Jendral Ahmad Yani 13 Ulu Palembang, 30263, Indonesia

<sup>2</sup> Department of Chemical Engineering, Faculty of Engineering, Sriwijaya University, Jalan. Raya Indralaya – Prabumulih KM. 32 Indralaya 30662, Ogan Ilir, Indonesia

<sup>3</sup> Department of Agricultural Industry Technology, Faculty of Agriculture, Sriwijaya University, Jalan. Raya Indralaya – Prabumulih KM. 32 Indralaya 30662, Ogan Ilir, Indonesia

<sup>4</sup> Department of Agricultural Industry Technology, Faculty of Agriculture, University of Lampung Jalan Soemantri Brojonegoro No.1, Bandar Lampung 35145, Indonesia

\* Corresponding author's e-mail: ariefkarim8@gmail.com

### ABSTRACT

Calcium carbide waste (CCW), the rest of the carbide welding workshop industry, is available in quite a lot and is immediately disposed of into the environment. Because CWW has a high pH value and a large specific surface area, it can act as an adsorbent in removing metals from groundwater. The content of metals in groundwater is indicated by a reddish color; however, upon contact with air, groundwater oxidation causes iron ions and manganese ions to precipitate. Synthetic groundwater was prepared in this experiment using reagents containing and . Observations were made in a batch process to assess the potential and ability of CCW to reduce iron and manganese levels in groundwater. In this study, to achieve equilibrium, CCW was mixed with 100 mL of synthetic solution and shaken at 25°C with a shaker. Operating time, levels of Fe(II) and (Mn(II) metals, and the mass of CCW were some of the parameters studied in this study. CCW was very good at reducing levels of iron ions and manganese ions after 60 minutes of operation. The percentage of removal of iron and manganese ions respectively – successively increased from 93.765 to 97.99% for iron ions and manganese ions from 91.83 to 95.14% for the initial concentration range of 40 mg/L, 60 mg/L, 80 mg/L, and 100 mg/L. Furthermore, the adsorption kinetics of CCW adsorbent in a mixture of iron ion and manganese ion solutions is a second-order kinetic equation. This confirms that the adsorption of CCW on iron ions and manganese ions is a chemisorption process. Calcium carbide waste has the potential to act as an absorbent of heavy metals in groundwater, especially iron and manganese ions.

**Keywords:** calcium carbide residual, iron, manganese, groundwater.

### INTRODUCTION

Groundwater contamination is one of the urgent problems faced by the availability of clean water sources at this time and will get worse in the future. This can be due to increased activities in the household sector industrialization, and both the chemical and mining industries which can contaminate groundwater. [Al. Sudan, 2018; D. Han and colleagues, 2016]. Groundwater contamination is caused by the presence of mineral or rock elements in the earth's crust, such as iron

(II) and manganese (II) metal compounds. When iron and manganese compounds dissolve and reach the groundwater table, they become insoluble and change the color of the water to brown or reddish [Esfandiar et al, 2014]. Iron and manganese in small concentrations can cause a variety of problems, including the formation of iron oxide deposits in the pipes, discolored water, and an unpleasant metallic taste. At higher concentrations, it causes health, aesthetic, and economic problems, as well as possible Parkinson's effects. [AlHobaib et al., 2016; Esfandiar et al., 2014].

The content of iron and manganese contained in groundwater before being used as drinking water must be removed or reduced first. The content of elements of iron (II) and manganese (II) in drinking water must be less than 0.3 mg/L and 0.05 mg/L, respectively. [WHO 2011]

Reducing heavy metal elements in groundwater can be used in several ways, including an advanced oxidation process [J.A. Khan et al., 2013], ion exchange [Arshid Bashir et al. 2018; Abdennebi et al., 2017; Ihsanullah et al., 2016], membrane separation [Du et al., 2019] and reverse osmosis [Sayed M et al., 2012], chemistry Of the several existing methods, the adsorption method is one of the well-known, efficient, technological inexpensive, safe and inexpensive water treatment to remove iron and manganese content in groundwater [Liu et al., 2016; Yang, X et al., 2019]. Given that this adsorption method is relatively simple to implement, it is necessary to identify an inexpensive material suitable for use as an adsorbent. Metal oxide and hydroxide-based adsorbents have been used to remove naturally occurring organic matter and their constituents from water [Bhatnagar and Sillanpää., 2017]. Potential materials that can be used as adsorbents from environmentally friendly natural materials or industrial waste. The material must have a large surface area, large pore size, and large internal volume.

The solid waste generated from the rest of the welding process is very abundant. CCW is a by-product of the acetylene gas ( $C_2H_2$ ) production process. CCW is usually disposed of as waste, posing a threat to the environment. The main component of CCW contains the elements  $Ca(OH)_2 = 92\%$ ,  $CaCO_3 = 2.9\%$ , and  $SiO_2 = 1.32$ , as well as elements of sulfides, metal oxides, and organic matter (Sun et al., 2015).

Organic compounds left over from the combustion of the carbide welding industry have a very high degree of acidity (alkaline), with a pH of 12.84, specific gravity (Gs) of 2.32, a specific surface area of 24,664  $m^2/g$ , clay particle size distribution (0.002 mm); silt (0.002 to 0.074 mm); and (>0.074 mm), according to Jiang et al. (2016). CCW can be used as an adsorbent in groundwater treatment because of these properties. So far, not many studies have used CCW as an adsorbent in the adsorption process to remove iron (II) and manganese (II) elements contained in groundwater. The purpose of this study was to determine the potential of CCW to remove iron(II) and manganese(II) contained in groundwater through

an adsorption process. Observations were made using a batch test, namely, the effect of several parameters on the ability of CCW in the adsorption process, including adsorbent dose, initial concentration, and contact time, which were analyzed using first-order and second-order kinetic models.

## RESEARCH METHODOLOGY

### Preparation of calcium carbide residue absorbent

The material used as an adsorbent in this study was calcium carbide solid waste resulting from the welding process. The steps taken are: The waste resulting from the carbide welding process is in the form of wet lumps, then dried by drying naturally, then after the calcium carbide solid waste is dry, it is sieved with a size of 80 mesh then soaked in Aqua DM for 24 hours, drained and printed in tablet form as shown in Figure 1. After that, it is dried and the adsorbent can be used, the weight of one adsorbent tablet is 0.45 gr.

### Analysis of adsorbent functional group characteristics

To determine the characteristics and functional groups of CCW, a Fourier Transform Infra-Red (FTIR) test was performed, using a Shimadzu spectrophotometer with a medium infrared spectrum (wave number 400–4000  $cm^{-1}$ ).

### Synthetic waste production

In this experiment, synthetic solutions of elements iron (II) and manganese (II) were used using and salts which were dissolved in distilled water. With each concentration of 100 mg/L. with variations in the mass of the adsorbent ranging from 5–180 minutes.

### Batch adsorption experiments

This research was conducted to study the characteristics of CCW in absorbing iron (II) and manganese (II) elements in groundwater. Tests were carried out by varying the dose of CCW, namely 2.5 to 7.5 g, the initial conditions for the two metal elements were the same, namely 40 mg/L, 60 mg/L, 80 mg/L, and 100 mg/L. with a time variation of 5 to 180 minutes. To determine the

optimum conditions carried out using the batch adsorption method, the solution obtained was filtered and then analyzed using AAS Shimadzu (ASS-3600), at a wavelength of 280 nm.

#### Analytical method

To find out the equivalence values of iron (II) and manganese (II) elements on the adsorbent surface that occur every time ( $q_t$ ) is calculated in Equation [Javadian et al., 2015]:

$$q_e = \frac{(C_0 - C_e) V}{M} \quad (1)$$

where: – the adsorbed metal state at equivalence (mg/L),  $C_0$  – the initial state before the adsorption process (mg/L),  $C_e$  – the final state after the adsorption process (mg/L),  $M$  – the mass of CCW (g) and  $V$  – the volume of the adsorbate (L). To calculate the percent removal, use the following formula [Wan et al., 2010; Abu et al., 2013]:

$$\left\{ \frac{(C_0 - C_e)}{C_0} \right\} \times 100\% \quad (2)$$

#### Adsorption kinetics

The kinetic model is used to understand the absorption rate that occurs in the adsorbent in the adsorbate. There are two kinetic models commonly used for solid-liquid adsorption processes, namely first-order and second-order pseudo-kinetic models [Yahaya et al., 2011]. First-order kinetic equations to find the process rate constant, as stated below.

$$\ln(q_e - q_t) = \ln q_e - k_1 t \quad (3)$$

where:  $q_e$  and  $q_t$  – represent the amount of metal ion adsorbed at equilibrium and in the final state  $t$  (time), (mg/L), (min-1) – the pseudo-first-order kinetic constant. The first-order kinetic model equations are all as follows.

For pseudo-second-order kinetic equations, it can be expressed as [Ho, 2006].

$$\frac{t}{q_t} = \frac{1}{k_2 q_e^2} + \frac{1}{q_e} t \quad (4)$$

To calculate the absorption rate ( $h$ ) can be used Equation 5.

$$h = k_2 q_e^2 \quad (5)$$

where:  $h$  – can be said to represent the initial adsorption rate constant at  $t = \text{zero}$  (mg/g.min), and – the amounts of adsorbed metal

ions at equilibrium (mg/g) and at time  $t$  (minutes), is the value of the second order kinetic rate constant (mg/g.hours). – can be obtained from each slope and the intersection between  $t/q$  versus  $t$ . When plotting  $t/q_t$  against  $t$ , a straight line is obtained.

## RESULTS AND DISCUSSIONS

### Characterization of CCW before and after adsorption with FTIR

Analysis of Functional Group Characteristics of Adsorbent FT-IR spectra test on the adsorbent was carried out to determine the functional groups present in the adsorbent. In this study, the FT-IR used was a Shimadzu spectrophotometer with a medium infrared spectral range (wave number 400-4000  $\text{cm}^{-1}$ ). The FTIR test shows that there is an absorption peak of the % transmittance spectrum (Y-axis) that extends over several waves (X-axis). FTIR test results on adsorbents without activation produce functional groups in Figure 1.

In Figure 1, the trend of the FTIR spectrum shows several main peaks that are almost the same. It can be seen that each type of active substance has almost the same range of wave numbers. Several peaks form in the range 2800–2900  $\text{cm}^{-1}$ , 1500–1650  $\text{cm}^{-1}$ , and then 1000–1200  $\text{cm}^{-1}$ . According to Liang et al. 2010, Vibration strains at bandwidths between 3400–3800  $\text{cm}^{-1}$  indicate the presence of active site vibrations containing O-H from alcohols, phenols, and carboxylic acids. The several peaks observed in the spectrum indicate that the calcium carbide residue has hydroxyl groups that reach the hydroxyl peak. the peak of the active site that can bind to the cation. Absorption at vibrations of 3637.9  $\text{cm}^{-1}$  indicates the presence of CaO, this indicates a correlation with the presence [Jitjamnong et al., 2019]. The wavelength of 3391.9  $\text{cm}^{-1}$  shows vibrations on the active site which corresponds to the hydroxyl strain and functions for OH bonds and forms the structure of the Ca(OH)<sub>2</sub> OH group from alcohol, phenol, and carboxylic acids [Huang and Zhu, 2012; Huang et al., 2014; Li Y et al., 2014, Mar and Somsook, 2012]. The presence of a peak band as high as 633.63  $\text{cm}^{-1}$  indicates the presence of Fe-O groups [Rachel et al., 2015]. For the functional group peak as high as 715  $\text{cm}^{-1}$  is the band associated with the Mn-O vibrational strain on manganese. Furthermore, the

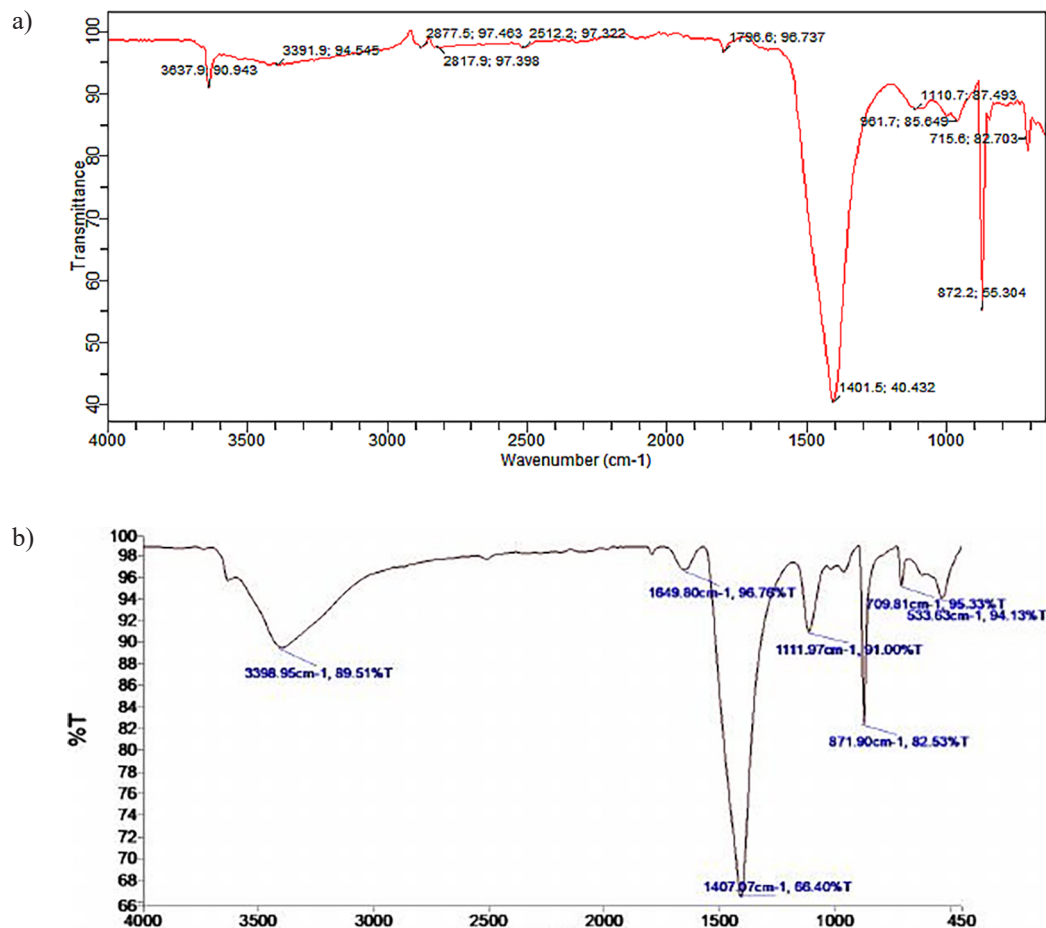


**Figure 1.** FTIR test results of CCW adsorbents (A) and (B) before and after the adsorption process respectively

absorption peaks at wavenumbers near 1236 and 812  $\text{cm}^{-1}$  represent the  $-\text{OH}$  surface of the Mn-OH group [Gotic et al., 2013]. The presence of hydroxyl groups in the CCW adsorbent can be concluded that the CCW adsorbent is good for reducing the content of iron (II) and manganese (II) elements in groundwater.

### Morphological structure of CCW as an adsorbent

To determine the active surface structure and particle size of CCW before and after being used as an adsorbent in the process of reducing the content of iron (II) and manganese (II) in groundwater, was carried out using SEM (Scanning Electron Microscopes) with 500 times magnification as shown in Figure 2. Based on the results of SEM analysis, it appears that there is a change in surface texture and pore development in CCW. It appears that the surface of the CCW is rough and uneven in the form of small pores. In Figure 2a it can be seen that the CCW surface is clean and clear with several macro pores, so it has

a higher ability to absorb metal ions. Figure 2b shows some macropores formed by small irregularly spherical flake particles with a size of 2  $\mu\text{m}$ .

### Elemental composition analysis of calcium carbide residue

To determine the residual elemental content of calcium carbide, analytical characterization was carried out using energy-dispersive X-ray spectroscopy techniques. EDX analysis provides a spectrum showing peaks that correlate with the elemental composition of the calcium carbide residue. Table 1. Shows the results of the analysis of the chemical composition contained in the calcium carbide residue before and after being used as an adsorbent. The characterization results using SEM-EDX to reduce the content of iron (II)

metal ions and manganese (II) metal ions are shown in Figure 3. The results obtained were in the form of the remaining percentage of the calcium carbide adsorbent component. Table 1 shows the recapitulation of the adsorbent composition. Based on the results of the EDX analysis

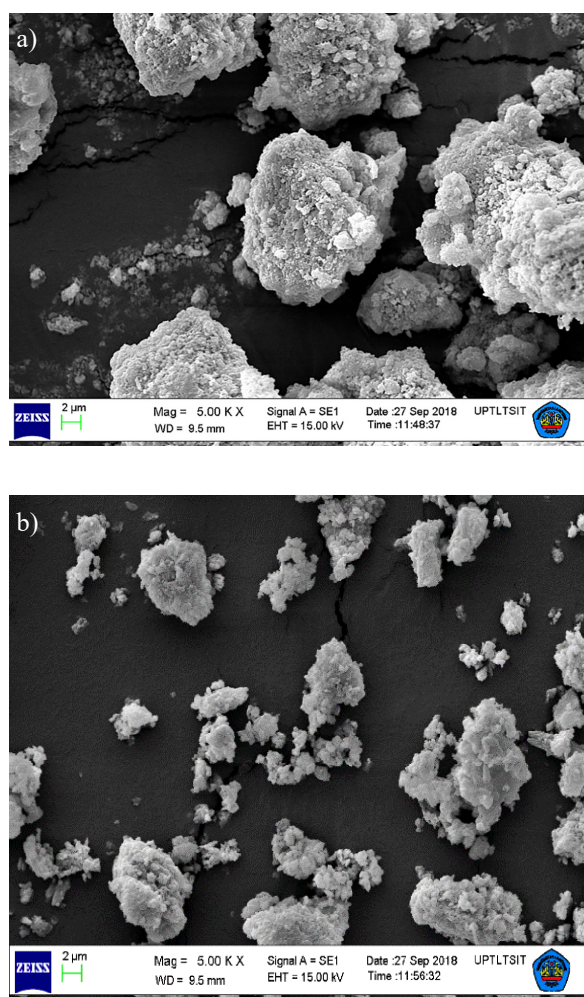


**Figure 2.** SEM analysis results on CCW (a) before and (b) after being used for the adsorption process of metals (Fe and Mn) in groundwater

presented in table 1 it can be seen that the adsorption process of groundwater with CCW contained only 3.92% Manganese Oxide (MnO), this indicates that CCW's ability to bind manganese (II) ions is not good. when compared with the ability of CCW to bind iron (II) at 9.20%. Manganese

oxide is formed from the adsorption process of groundwater, with the reaction occurring to form which can be used to bind manganese from water. In this process, a monovalent cation is formed due to the presence of quite a lot of in solution which is usually released from the medium to form Mn bonds, so bicarbonate compounds tend to become carbonate compounds because Mn(II) is selectively reduced to MnO.

### Contact time on the adsorption process

Contact time is one of the important factors that must be studied in the adsorption process. Choosing the right contact time for metal-containing groundwater treatment processes certainly has economic advantages. From the observations, the effect of contact time on the metal adsorption process in groundwater using CCW is shown in Figure 4.

In Figure 4 it can be seen that the absorption of the two metals by CCW took place quickly, and Fe(II) saturation was reached around the 90th minute while Mn was reached around the 120th minute. This time indicates that the adsorption process of iron (II) and manganese (II) ions reached stable conditions until the end of the process. In this condition there is no longer the amount of adsorbate that is adsorbed, this condition is known as the equilibrium condition.

### Effect of initial pH of synthetic solutions

At this stage, changes in the initial pH were observed for the rate of decrease in the levels of synthetic iron (II) and manganese (II) during the adsorption process with CCW. At this stage, the pH of the solution ranged from pH 2.5 to 8. The initial concentration of iron (II) and manganese (II) ions was set at 100 mg/L and the mass of

**Table 1.** The chemical composition of CCW before and after it is used as an adsorbent in the adsorption process

NO	Component	Composition (% by weight)	
		Before adsorption	After adsorption
1	Carbon, C	13.84	26.19
2	Alumina, Al <sub>2</sub> O <sub>3</sub>	2.38	2.64
3	Silica dioxide, SiO <sub>2</sub>	2.61	1.23
4	Sulfites, SO <sub>3</sub>	1.65	4.33
5	Calcium oxide, CaO	79.53	52.49
6	Iron(II) oxide, FeO	-	9.20
7	Manganese oxide, MnO	-	3.92
8	Total	100	100

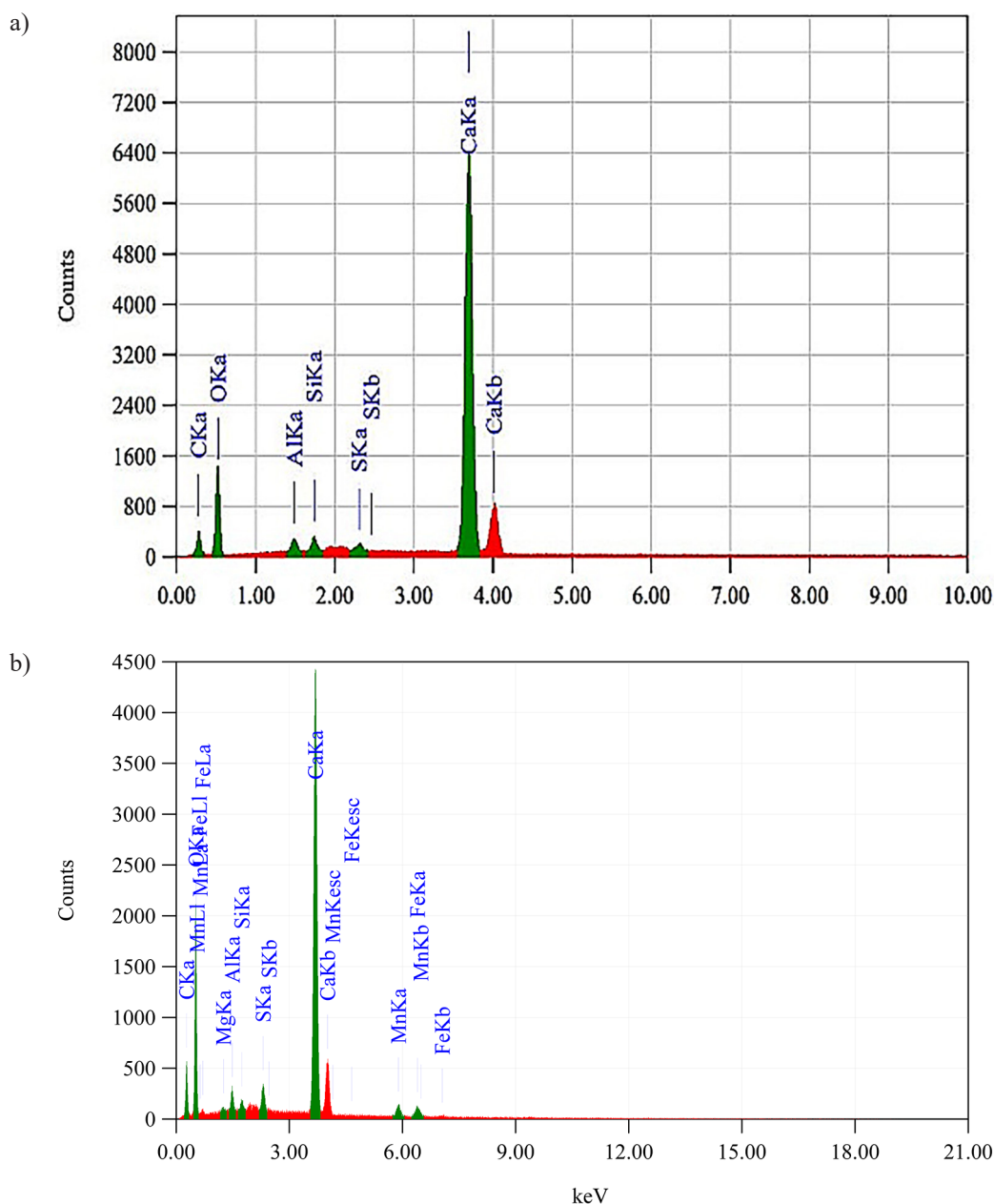


**Figure 3.** SEM-EDX analysis of CCW adsorbents (a) before and (b) after being used for batch adsorption of metal ions (Fe and Mn) in groundwater

CCW was 5 g. Figure 5 shows that the change in the pH value reduces the levels of iron (II) and manganese (II) within 120 minutes. Under these conditions, the percentage of removal of each metal increased for both iron (II) and manganese (II), which increased from 93.76% to 97.99% and from 91.83% to 95.14%. The increase was due to the charge exchange on the surface of the adsorbent with an increase in the pH value. In addition, the pH of the solution also regulates the ionization level of adsorbed metals during the process [El Qaeda et al, 2006]. The maximum removal of iron (II) was seen at pH 6 to pH 8,

where the pH range did not change significantly from 97.99 to 98.91% for iron (II) ions while for manganese(II) ions, there was no significant change, namely 95.14% at pH 6, to 95.21% at pH 8. This phenomenon may be partly due to an increase in the pH value causing the outer layer of the adsorbent to be charged with negative ions so that the metal ions are attracted towards the positive. This increase is probably due to the formation of hydroxyl complex ions or metal cation hydrolysis solutions [Badmus et al., 2007]. As a result, the adsorption on the CCW surface also increases.

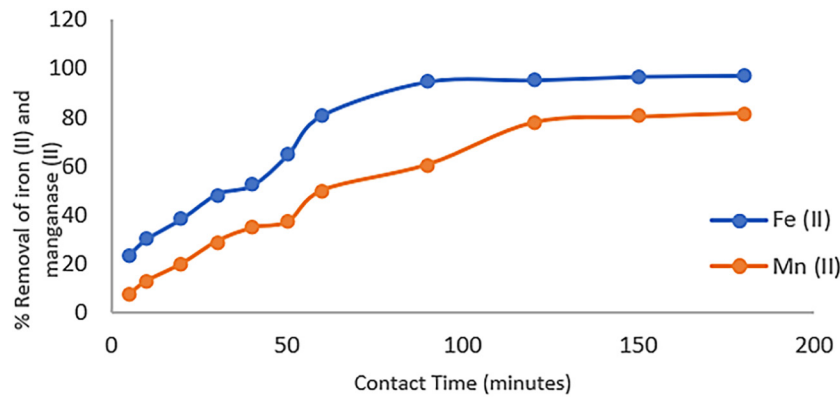


**Figure 4.** Relationship between contact time and adsorption of metal ions (Fe and Mn) in groundwater on CCW

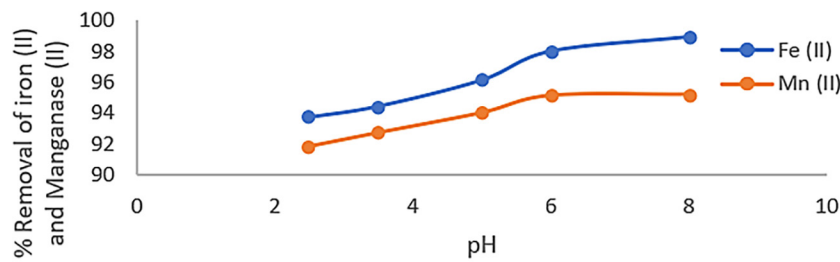


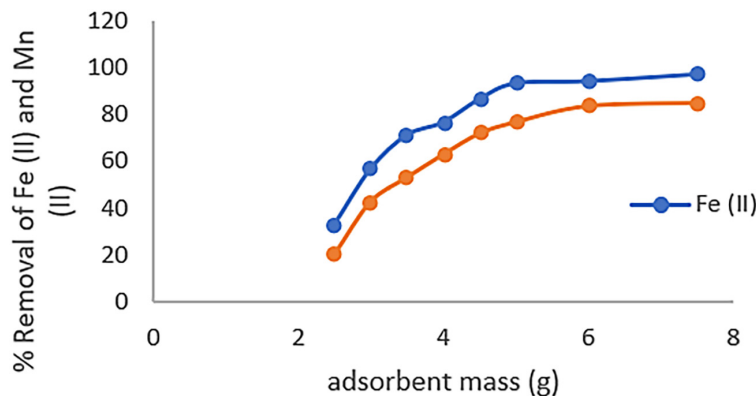
**Figure 5.** Effect of initial solution pH on the percentage removal of iron (II) and manganese (II) ions

**The effect of changing the dose of CCW**

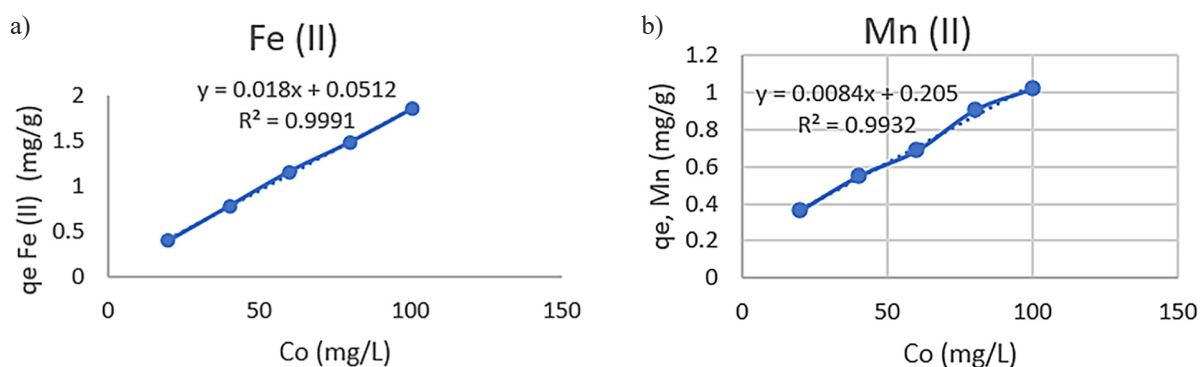
Studies on changes in CCW doses are needed to determine the optimal dose of CCW needed to remove metal ions from groundwater. Experimental data related to the change in CCW dose to the percentage reduction in the concentration of iron (II) and manganese (II) ions in groundwater is shown in Figure 6.

Figure 7 shows that increasing the mass of the adsorbent from 2.5 g to 7.5 g can increase the percentage reduction in the concentration of metal ions in synthetic solutions (Fe II and Mn II). Increase in the percentage of absorbed iron

(II) ions from 33.16% to 96.78%. Meanwhile, manganese(II) ions increased from 20.06% to 84.98%. The efficiency of reducing iron(II) ions increases exponentially with increasing the mass of the adsorbent from 2.5 to 5 g, while the adsorption efficiency of Mn(II) ions increases with changing the mass of the adsorbent from 2.5 to 6 g. At a higher adsorbent mass of up to 7.5 g, the two removals were nearly the same, this was due to the availability of active sites on the surface due to the increased mass of the CCW adsorbent. The maximum point of adsorption occurred at 96.78% for iron (II) metal ions and 84.98% for manganese (II) metal ions. This is because when



**Figure 6.** Effect of changing the dose of CCW on the percentage reduction of iron (II) and manganese (II) ions



**Figure 7.** Relationship Effect of initial solution conditions on heavy metal adsorption by CCW (5 g in 100 ml solution, 180 minutes) (a) Fe(II) (b) Mn(II)

**Table 2.** Effect of initial solution concentration on the adsorption capacity of CCW

Heavy metals	Initial concentration, Co (mg/L)	Amount absorbed, $q_e$ (mg/g)	Percentage absorbed R (%)	Heavy metals	Initial concentration, Co (mg/L)	Amount absorbed, $q_e$ (mg/g)	Percentage absorbed R (%)
Fe (II)	20	0.396	99.1	Mn (II)	20	0.365	91.2
	40	0.778	97.25		40	0.544	68.75
	60	1.162	96.83		60	0.688	57.33
	80	1.485	92.8		80	0.906	56.63
	100	1.847	92.35		100	1.028	51.1

the adsorbent dose reaches a certain level in the adsorption process, the existing particles tend to decrease to absorb more metal ions onto the surface of the adsorbent so that the rate of removal of metal ions in groundwater is difficult to continue. (Onundiet et al., 2010)

Tabulation of the regression coefficient  $R^2$  obtained for the adsorption processes of iron (II) metal ions and manganese metal (II) ions is presented in Table 3. Table 3 shows the suitability for applying the second-order pseudo-adsorption kinetics model. Adsorption kinetics are not suitable for pseudo-first-order kinetic models because all  $R^2$  are less than 0.9. Meanwhile, the pseudo-second-order kinetic model is very suitable based on the experimental data obtained, namely all  $R^2$  close to one, namely 0.95. These findings indicate that the adsorption process of ferrous (II) and manganese

(II) metal ions in groundwater synthetic wastewater solutions can be controlled by film dimensions or a combination of film and surface adsorption.

Meanwhile, the first-order pseudo-kinetic model shows that the absorption rate is limited by one process or mechanism that acts on one adsorbent site (Mondal et al., 2008). According to Table 3 and Figure 8, pseudo-order one does not provide an accurate adsorption capacity. Furthermore, the value of  $R^2$  is relatively less linear. Consequently, the pseudo-first-order kinetic model cannot describe the entire adsorption process onto a heterogeneous surface. However, the second-order pseudo-kinetic model shown in Figure 9 is more precise and linear than the first-order pseudo-kinetic model. The regression coefficients obtained using a pseudo-second-order kinetic model, namely 0.99 for ferrous (II) and manganese (II)

**Table 3.** Relationship between kinetic constants and CCW adsorption rates

Systems	Heavy metal	Pseudo-First-Order Coefficients			Pseudo-Second-Order Coefficients		
		$q_e$ , Kalk	$k_1$	$R^2$	$q_e$	$k_2$	$R^2$
Single	Fe (II)	4.98	0.219	0.984	90	0.971	0.99
	Mn (II)	1.487	0.023	9.91	1.981	0.0017	0.99
Binary	Fe (II)	1.785	0.025	0.8652	2.371	0.0123	0.947
	Mn (II)	1.306	0.025	0.9053	2.627	$3.37 \times 10^{-3}$	0.950



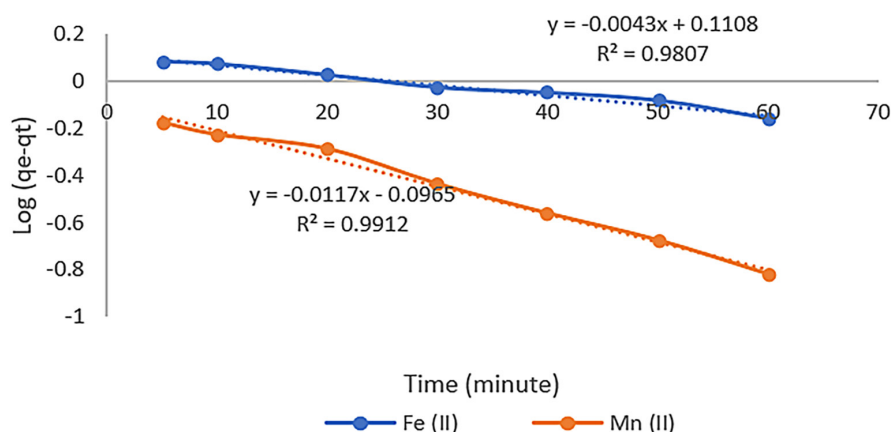


**Figure 8.** Relationship between pseudo-first-order kinetic model and CCW adsorption rate

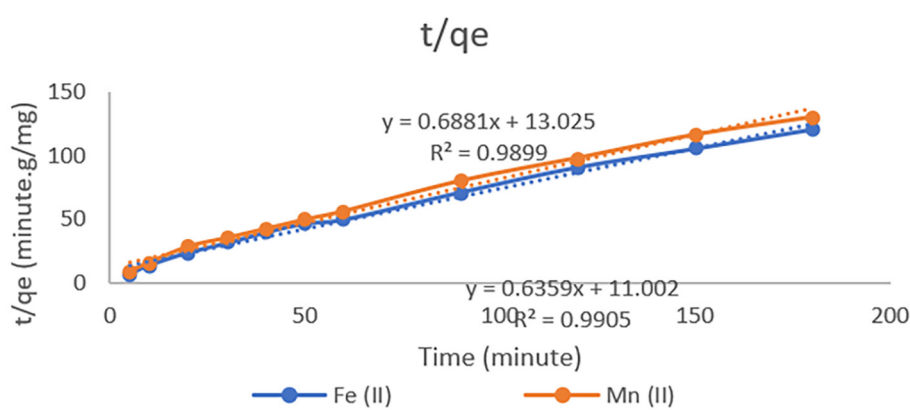


**Figure 9.** Relationship between pseudo-second-order kinetic model and CCW adsorption rate

metal ions, show this. These results indicate that the adsorption of iron (II) and manganese (II) ions onto the rest of the calcium carbide adsorbent follows a pseudo-second-order kinetics model equation, confirming that the adsorption of iron (II) and manganese (II) ions on the CCR is a chemisorption process. Following the adsorption kinetics process for the pseudo-second-order kinetics model equation, Mohan et al. (2012) predicted that the overall rate of adsorption of iron (II) and manganese (II) metal ions on CCW seemed to involve a chemical reaction or electron exchange between the adsorbent and the adsorbate. This is because the CCW adsorbent contains calcium ions which can act as materials for the ion exchange process.

## CONCLUSION

The results of this study can be concluded that solid waste calcium carbide is suitable as an adsorbent to reduce the concentration of iron (II) ions. The adsorption kinetics of iron (II) ions on the

remaining calcium carbide adsorbent correspond to the pseudo-first-order adsorption kinetics. The adsorption kinetics of manganese (II) ions on the calcium carbide residue adsorbent tends to follow the pseudo-second-order kinetics model so that the adsorption process that takes place on manganese (II) metal ions by the calcium carbide residue adsorbent is chemical adsorption (chemisorptions).

The adsorption kinetics of a mixture of iron (II) metal ions and manganese (II) metal ions on the calcium carbide residue adsorbent tends to follow the pseudo-second-order kinetics model which confirms that the adsorption process is a chemisorption process. The order of selectivity of the CCW adsorbent to ferrous metal ions (II) is higher than that of manganese(II) metal ions.

## REFERENCES

1. Abdennebi N., Benhabib K., Goutaudier C., Bagane M. 2017. Removal of Aluminium and Iron Ions from Phosphoric Acid by Precipitation of Organo-Metallic

- Complex Using Organophosphorous Reagent. *Journal of Materials and Environmental Science*, 8, 557–565.
2. Abuh M.A., Akpomie G.K., Nwagbara N.K., Abia-Bassey N., Ape D.I., Ayabie B.U. 2013. Application of Kinetic Rate Equation on Copper (II) and Zinc (II) Removal with Lignocellulosic Fibers Without Layer Modification Palm Tree Trunk Single Component System Study. *International Journal of Basic and Applied Sciences*, 50, 800–809.
  3. Abuh M.A., Akpomie G.K., Nwagbara N.K., Abia-Bassey N., Ape D.I., Ayabie B.U. 2013. Kinetic Rate Equations Application on the Removal of Copper (II) and Zinc (II) by Unmodified Lignocellulosic Fibrous Layer of Palm Tree Trunk-Single Component System Studies. *International Journal of Basic and Applied Sciences*, 50, 800–809.
  4. Al-Hobaib A.S., Al-Sheetan Kh.M., El Mir L. 2016. Effect of iron oxide nanoparticles on the performance of polyamide membrane for groundwater purification. *Mater Sci Semicond Process* 42(Part 1), 107–110.
  5. Al-Sayed M. Aly., Mahmoud M.K., Hamdy A., Khaled Z.M., Mohamed A.B. 2012. Reverse Osmosis Pretreatment: Removal of Iron in Groundwater Desalination Plant in Shupramant-Giza - A Case Study. *Current World Environment*, 7(1), 23–32.
  6. Amirnia S., Ray M.B., Margaritis A. 2016. Copper Ion Removal by *Acer saccharum* Leaves in a Regenerable Continuous-Flow Column. *Chemical Engineering Journal*, 287, 755–764.
  7. Arshid B., Lateef A.M., Sozia A., Taniya M., Mudasir A.B., Dar G.N. 2018. Altaf Hussain Pandith1 Removal of heavy metal ions from aqueous system by ionexchange and biosorption methods. *Environmental Chemistry Letters*.
  8. Barloková D., Ilavský J. 2009. Removal of Iron and Manganese from Water Using Filtration by Natural Materials. *Polish J of Environ*, 19(6), 1117–1122.
  9. Bhatnagar A., Sillanpää M. 2017 Removal of Natural Organic Matter (NOM) and Its Constituents from Water by Adsorption—A Review. *Chemosphere*, 166, 497–510.
  10. Dongmei H., Matthew J.C. 2016. Guoliang Cao cDeep challenges for China's war on water pollution. *Environmental Pollution*, 218, 1222–1233.
  11. Esfandiari N., Nasernejad B., Ebadi T. 2014. Removal of Mn(II) from groundwater by sugarcane bagasse and activated carbon (a comparative study): Application of Response Surface Methodology (RSM). *J. Ind. Eng. Chem.*, 2, 3726–3736.
  12. Gotić M., Jurkin T., Musić S., Unfried K., Sydlík U., Bauer-Šegvić A. 2013 Microstructural Characterization of Different Mn-Oxide Nanoparticles Used as Models in Toxicity Studies. *Journal of Molecular Structure*, 1044, 248–254.
  13. Hongfang S., Zishanshan L., Jing B., Shazim A.M., Biqin D., Yuan F., Weiting Xu., Feng X. 2015. Properties of Chemically Combusted Calcium Carbide Residue and Its Influence on Cement Properties. *Materials*, 8, 638–651.
  14. Hosseini H., Rezaei H., Shahbazi A., Maghsudlu A. 2016 Application of Nano-Lignocellulose to Remove Nickel Ions from Aqueous Solutions. *Environmental Resources Research*, 4, 213–229.
  15. Huang K., Zhu H.M. 2012. Removal of Pb<sup>2+</sup> from aqueous solution by adsorption on chemically modified muskmelon peel. *Environ Sci Pollut Res*. DOI: 10.1007/s11356-012-1361-7
  16. Ihsanullah, Aamir A., Adnan M., Al-Amer, Tahar L., Mohammed J.A.M., Mustafa S.N, Majeda K., Muataz A.A. 2016. Heavy metal removal from aqueous solution by advanced carbon nanotubes: Critical review of adsorption applications. *Separation and Purification Technology*, 157, 141–161.
  17. Khan J.A., He X., Khan H.M., Shah N.S. 2013. Dionysiou, Oxidative degradation of atrazine in aqueous solution by UV/H<sub>2</sub>O<sub>2</sub>/Fe<sup>2+</sup>, UV//Fe<sup>2+</sup> and UV//Fe<sup>2+</sup> processes: a comparative study. *Chem. Eng. J.*, 218, 376–383.
  18. Javadian H., Ghorbani F., Tayebi H., Asl S.H. 2015. Study of Adsorption of Cd(II) from Aqueous Solutions Using Zeolite-Based Geopolymers, Synthesized from Coal Fly Ash; Kinetic Studies, Isotherms, and Thermodynamics. *Journal of Arabic Chemistry*, 8, 837–849.
  19. Jawed A., Pandey L.M. 2019. Application of bimetallic Al-doped ZnO nano-assembly for heavy metal removal and decontamination of wastewater. *Water Sci. Technol.*, 1–12
  20. Jiang H.X., Sunb Q., Zhang L.L., Zhao J.Z., Al-Ti-C. 2018. Master alloy with nano-sized TiC particles dispersed in the matrix prepared by using carbon nanotubes as a C source. *J. Alloys Compd.*, 748, 774–782.
  21. Al-Sudani H.I.Z. 2018. Hydrochemical Evaluation and Utilization of Groundwater. Khanaqin Area, Diyala Governorate - East of Iraq. *Iraqi Journal of Science*, 59(4C), 2279–2288.
  22. Kai H., Yifan X., Hongmin Z. 2014 Removal of heavy metal ions from aqueous solution by chemically modified mangosteen pericarp. *Desalination and Water Treatment*, 52, 7108–7116.
  23. Liu, H.Y., Guo, H.M., Xing, L.N., Zhan, Y.H., Li, F.L., Shao, J.L., N, H., L, X., Li, C.Q. 2016. Geochemical behaviors of rare earth elements in groundwater along a flow path in the North China Plain. *Journal of Asian Earth Sciences*, 117, 33–51.
  24. Lo S., Wang S., Tsai M., Lin L. 2012. Adsorption capacity and removal efficiency of heavy metal ions by Moso and Ma bamboo activated carbons. *Chemical Engineering Research and Design*, 90, 1397–1406.

25. Nik N., Daud N., Nur H. 2013. Improving Groundwater Quality using the Aeration and Filtration Method in Selangor, Malaysia. *International Journal of Environmental and Ecological Engineering*, 7(6), 309–313.
26. Piuleac C.G., Sáez C., Cañizares P., Curteanu, S. 2012. Hybrid Model of a Wastewater-Treatment Electrolytic Process. *International Journal of Electrochemical Science*, 7, 6289–6301.
27. Richard J., Debus. FTIR studies of metal ligands, networks of hydrogen bonds, and water molecules near the active site Mn4CaO5 cluster in Photosystem II. *Biochimica et Biophysica Acta (BBA) - Bioenergetics*, 1847, 19–34.
28. Wan M.W., Kan C.C., Rogel B.D., Dalida M.L.P. 2010. Adsorption of copper (ii) and lead (ii) ions from aqueous solution on chitosan-coated sand Carbohydr. Polym, 80, 891–899.
29. WHO. 2011. Guidelines for Drinking Water Quality. World Health Organization, Geneva, Switzerland. [http://apps.who.int/iris/bitstream/10665/44584/1/9789241548151\\_eng.pdf](http://apps.who.int/iris/bitstream/10665/44584/1/9789241548151_eng.pdf)
30. Xiaodong Y., Yongshan W., Yulin Z., Feng H., Zebin Y., Jun H., Hailong W., Yong S.O., Yinshan J., Bin G. 2019. Surface functional groups of carbon-based adsorbents and their roles in the removal of heavy metals from aqueous solutions: a critical review. *Chem. Eng. J.*, 366, 608–621.
31. Xing D., Guangyang L., Fangshu Q., Kai L., Senlin S., Guibai L., Heng L. 2019. Removal of iron, manganese, and ammonia from groundwater using a PAC-MBR system: The anti-pollution ability, microbial population, and membrane fouling. *Desalination*, 403, 97–106.